A PROGRESSIVE FAILURE MODEL FOR COMPOSITE LAMINATES WITH INITIAL DELAMINATION UNDER COMPRESSIVE LOADING

Yaling Liu[1], Libin Zhao[2], Kangkang Wang[3], Haiming Hong[4], Jianyu Zhang[5]

[1] School of Astronautics, Beihang University, Beijing 100191, PR China, sunlyl1995@buaa.edu.cn
[2] School of Astronautics, Beihang University, Beijing 100191, PR China, lbzhao@buaa.edu.cn
[3] School of Astronautics, Beihang University, Beijing 100191, PR China, wangkang@buaa.edu.cn
[4] Shenyang Aircraft Design & Research Institute, AVIC, Shenyang 110035, PR China, hhmzhs@hotmail.com
[5] College of Aerospace Engineering, Chongqing University, Chongqing 400044, PR China, jyzhang@cqu.edu.cn

Keywords: Composite laminates; Delamination; Compression; Progressive failure

ABSTRACT

Delamination is one of the most serious failure modes in laminated composites caused by factors such as manufacturing flaws, object impacts and fatigue loads. Composite laminates with initial delamination have attracted high attention because the delamination leads to a significant decrease of the load carrying capacity of the laminates under compression. In this paper, the compressive behavior of composite laminates with embedded delamination was investigated numerically and experimentally. A progressive failure model was established and nonlinear failure analyses were carried out, in which the intra-laminar failure was dealt with a progressive damage method and the interlaminar delamination growth was simulated with the virtual crack closure technique. The significant effects of delamination size on the compressive behavior, especially on the failure mechanism, were discussed. Furthermore, three typical failure criteria including the B-K criterion, Reeder criterion and Power-law were comparatively studied for accurately evaluating the crack propagation. Different model parameter set schemes were discussed to obtain a suitable numerical model for accurately predicting the failure of the laminates with embedded delamination.

1 INTRODUCTION

Carbon fiber reinforced composites are being extensively used in the fields of aerospace, aircraft, automotive, marine industries, etc., because of their attractive properties such as high specific stiffness and strength. However, due to the weakness of interlaminar behavior in composite laminates, delamination has become one of the most serious failure modes in laminated composites caused by factors such as manufacturing flaws, object impacts and fatigue loads and will lead to a significant decrease of the load carrying capacity of the laminates. Especially for composite laminates with initial delamination under a compressive loading, delamination growth often occurs coupling with buckling of delaminated sub-laminates, which exceedingly even catastrophically imperil the structural integrity and safety. Therefore, a deep understanding of the compressive failure behavior of the laminates with embedded delamination are extremely important.

Various sizes and shapes of composite flat laminates are studied by different authors. For numerical and experimental analysis, most existing researches have concentrated on slender rectangular composite laminates of which the length-width ratios are higher than 2 [1-7], while a few have concentrated on laminates of low length-width ratios [8, 9]. Given the standard experimental method ASTM D7137/ D7137M-07 well established for the compressive test of laminates with impact-induced delaminations, which is also often used to investigate the damage tolerance behavior of composite laminates, the size and shape of composite plates in this paper are in accordance with ASTM standard, in which the length-width ratio of the laminate equals to 1.5.

Numerical methods have been often employed to study the stability and delamination problems of composite laminates with initial delamination during past three decades, such as stress-based failure methods, virtual crack closure technique (VCCT) and cohesive element methods. The stress-based

failure methods have a severe dependency on mesh size owing to the stress singularity problem. Even though the cohesive element methods combine the strength-based failure methods with fracture mechanics, they have a strict demand for grid density and therefore are computationally demanding. In contrast, the virtual crack closure technique is not sensitive to the FEA mesh size, so it requires less computationally cost. Moreover, the virtual crack closure technique could intuitively extract the information of strain energy release rate (SERR), which is extensively used to predict and investigate the crack propagation. Based on the above considerations, it's of great importance to systematically investigate the compressive behavior of the laminate with embedded lamination using the virtual crack closure technique.

Currently, many efforts have been made on the effects of different parameters when using the virtual crack closure technique. Krueger and Goetze [10, 11] discussed the influence of parameters such as the element type, integration order, release tolerance and damage factor. Liu [3] studied the influence of parameters such as the element size, load step number, symmetry boundary conditions and failure criteria on the delamination growth of slender composite laminates with through-width delaminations. However, in the literature, almost no research study can be found which deals with the effects of different parameters on the delamination growth and buckling behavior in composite laminates with embedded delamination under compression. Thus, it's necessary to establish different models to obtain a suitable parameter set scheme for accurately predicting the failure of the laminates with initial delamination.

In this paper, the compressive behavior of composite laminates with embedded delamination was investigated numerically and experimentally. A progressive failure model was established and nonlinear failure analyses were carried out. According to the failure characteristics of the laminates with embedded delamination under compression, the intra-laminar failure in the laminates was dealt with a progressive damage method and the interlaminar delamination growth was simulated with the virtual crack closure technique. The significant effects of delamination size on the compressive behavior, especially on the failure mechanism, were discussed. Furthermore, three typical failure criteria including the B-K criterion, Reeder criterion and Power-law were comparatively studied for accurately evaluating the crack propagation. Different model parameter set schemes were discussed to obtain a suitable numerical model for accurately predicting the failure of the laminates with embedded delamination.

2 COMPRESSIVE TESTS

According to the statistical data, most of delaminations resulting from manufacturing flaws or use distribute in the deep locations, especially at $h/3$ and $h/2$. Delaminations of different geometric shape can be converted into circular ones for the ease of delamination production, and the size distribution of all delaminations is described as most of the diameters being smaller than Φ38.1 mm, some between Φ38.1 mm and Φ50 mm, whereas only a few bigger than Φ50 mm [8]. Based on the forementioned information, specimens with a lay-up of $(45/0/-45/90)_3(45/0)//(-45/90)(90/-45/0/45)_4$ were designed for static compressive tests, where the symbol '//' denotes the position of artificially induced circular delamination. Delaminations of three different sizes: Φ20 mm, Φ30 mm and Φ50 mm were introduced in the specimens, and a single thickness of 10 lm PTFE film was laid between plies to form the delamination [12]. For each kind of delamination size, three identical specimens were tested. The specimens were made of T300/QY8911 carbon-fiber bismaleimide prepreg with geometry dimensions of length l = 150 mm, width b = 100 mm and thickness h = 4 mm, as illustrated in Fig. 1. The mechanical properties of the composite materials obtained from the manufacturer are shown in Table 1.

The compression test was conducted in accordance with ASTM D7137/ D7137M-07. The position of strain gauges is shown in Fig. 1, which was used for measuring the axial strain and the compressive modulus. Out of plane deflections of the plate surfaces were recorded using two dial gages. At the beginning and end of the test, the ultrasonic C-scan method was employed to observe the shape of delamination. The actual experimental devices are shown in the Fig. 2. The ultrasonic C-scan method was employed to observe the shape of delamination before the start and the end of experimental period.

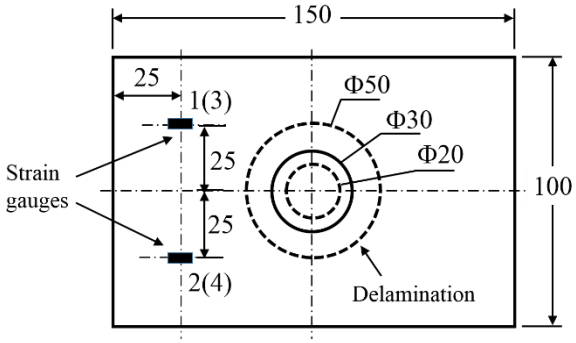

Figure 1: Geometry of a specimen with circular delamination.

Engineering constant		Identification	Engineering constant		Identification
E_{11}	[GPa]	131	X_T	[MPa]	1239
E_{22}	[GPa]	9.64	X_C	[MPa]	1081
E_{33}	[GPa]	9.64	Y_T	[MPa]	39
ν_{12}	–	0.3	Y_C	[MPa]	189
ν_{13}	–	0.3	Z_T	[MPa]	39
ν_{23}	–	0.3	Z_C	[MPa]	189
G_{12}	[GPa]	4.84	S_{12}	[MPa]	81
G_{13}	[GPa]	4.84	S_{13}	[MPa]	81
G_{23}	[GPa]	3.2	S_{23}	[MPa]	81
G_{IC}	[J/m^2]	252	G_{IIC}	[J/m^2]	665
G_{IIIC}	[J/m^2]	665			

Table 1: Material properties of T300/QY8911 composite.

Figure 2: Experimental devices.

3 FINITE ELEMENT MODEL

The ABAQUS software was used to carry out the finite element analysis. In the present study, the

finite element model was constructed with 8-nodes 3D solid elements. A typical finite element mesh and boundary conditions of the model are shown in Fig. 3. The support fixture has been modelled geometrically and fully constrained. The intra-laminar failure was dealt with progressive damage method and the delamination growth was simulated with the virtual crack closure technique.

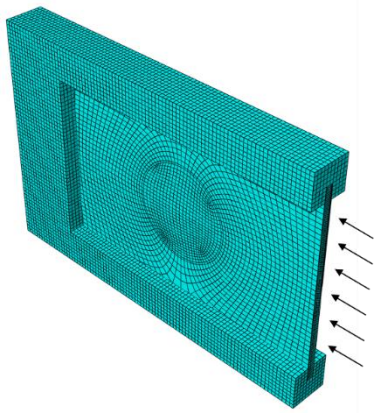

Figure 3: Finite element model.

The Hashin criteria [13, 14] have been adopted to evaluate the intra-laminar failure because it can distinguish different modes of failure such as failure of fiber and matrix in tension or compression. During the numerical process, the material properties are degraded at ply level according to the specific failure mode due to the implementation of criteria.

Several material properties degradation rules can be found in the literature [15-17]. An instantaneous degradation rule has been chosen in the present study, in which the material properties are multiplied by a degradation factor (k) in order to roughly estimate the stiffness loss. In this paper, the value of k is 0.05.

In Table 2, the Hashin criteria and corresponding properties degradation rules adopted are shown, where σ_{ij} are the stress components in the ij direction and S_{ij} are the material strengths respectively.

Failure modes	Failure criteria	Material property degradation
Fiber tension ($\sigma_{11}>0$)	$(\frac{\sigma_{11}}{X_T})^2+(\frac{\sigma_{12}}{S_{12}})^2+(\frac{\sigma_{13}}{S_{13}})^2\geq 1$	$E_1^{\,d}=kE_1$
Fiber compression ($\sigma_{11}<0$)	$(\frac{\sigma_{11}}{X_C})^2\geq 1$	$E_1^{\,d}=kE_1$
Matrix tension ($\sigma_{22}>0$)	$(\frac{\sigma_{22}}{Y_T})^2+(\frac{\sigma_{12}}{S_{12}})^2+(\frac{\sigma_{23}}{S_{23}})^2\geq 1$	$E_2^{\,d}=kE_2, \nu_{12}^{\,d}=k\nu_{12}, \nu_{23}^{\,d}=k\nu_{23}$ $G_{12}^{\,d}=kG_{12}, G_{23}^{\,d}=kG_{23}$
Matrix compression ($\sigma_{22}<0$)	$(\frac{\sigma_{22}}{Y_C})^2+(\frac{\sigma_{12}}{S_{12}})^2+(\frac{\sigma_{23}}{S_{23}})^2\geq 1$	$E_2^{\,d}=kE_2, \nu_{12}^{\,d}=k\nu_{12}, \nu_{23}^{\,d}=k\nu_{23}$ $G_{12}^{\,d}=kG_{12}, G_{23}^{\,d}=kG_{23}$
Fiber-matrix shear ($\sigma_{11}<0$)	$(\frac{\sigma_{11}}{X_C})^2+(\frac{\sigma_{12}}{S_{12}})^2+(\frac{\sigma_{13}}{S_{13}})^2\geq 1$	$\nu_{12}^{\,d}=k\nu_{12}, \nu_{13}^{\,d}=k\nu_{13}, \nu_{23}^{\,d}=k\nu_{23}$ $G_{12}^{\,d}=kG_{12}, G_{13}^{\,d}=kG_{13}, G_{23}^{\,d}=kG_{23}$

Table 2: Hashin criteria and Material degradation rules.

To simulate the delamination growth, the finite element models were established as two sublaminates, which were tied at the interface and can only debond when the computed stain energy rate is equal to or

greater than the critical strain energy release rate, except for the delamination area where contact conditions were used to prevent overlap of elements.

Various failure criteria have been reported in literature to account the crack propagation. Currently, three most typical criteria proposed to estimate damage growth initiation are used:

(1) B-K criterion [18]

$$G_{equC}=G_{IC}+(G_{IIC}-G_{IC})\left(\frac{G_{II}+G_{III}}{G_I+G_{II}+G_{III}}\right)^{\eta} \tag{1}$$

(2) Reeder criterion [19]

$$G_{equC}=G_{IC}+(G_{IIC}-G_{IC})\left(\frac{G_{II}+G_{III}}{G_I+G_{II}+G_{III}}\right)^{\eta}+(G_{IIIC}-G_{IIC})\left(\frac{G_{III}}{G_{II}+G_{III}}\right)\left(\frac{G_{II}+G_{III}}{G_I+G_{II}+G_{III}}\right)^{\eta} \tag{2}$$

(3) Power criterion [20]

$$\frac{G_{equ}}{G_{equC}}=\left(\frac{G_I}{G_{IC}}\right)^{a_m}+\left(\frac{G_{II}}{G_{IIC}}\right)^{a_n}+\left(\frac{G_{III}}{G_{IIIC}}\right)^{a_o} \tag{3}$$

In these criteria, G_{IC}, G_{IIC} and G_{IIIC} are critical strain energy release rate (SERR) for mode-I, mode-II and mode-III crack propagation. η, a_m, a_n and a_o are constants respectively.

In this study, the B-K criterion has been adopted to simulate the inter-laminar failure of the laminates with Φ20 mm, Φ30 mm and Φ50 mm circular delamination, and three typical failure criteria were comparatively studied for accurately evaluating the crack propagation of the laminate with Φ50 mm circular delamination.

4 VALIDATION AND ANALYSIS

The experimental results and numerical predictions of failure load are shown in Table 3 for the laminates of different delamination sizes. The failure loads decrease as the delamination size increases because the extremely large delamination size results in a decrease in the plate resistance against the buckling behavior [21].

Delamination size (mm)	Failure loads (kN)					Difference (%)
	Specimen 1	Specimen 2	Specimen 3	Average	FE prediction	
Φ20	148.20	151.90	151.80	150.63	153.77	2.08
Φ30	141.40	141.60	139.80	140.93	135.28	4.01
Φ50	109.10	107.30	109.20	108.53	105.21	3.06

Table 3: The comparison of the experimental results and FE prediction of failure load.

The comparison between experimental and predicted load-central deflection behavior for the laminates with Φ20 mm, Φ30 mm and Φ50 mm circular delamination are shown in Fig. 4 (a), (b) and (c), respectively. Generally, delaminated composite laminates experience three main buckling stages: non-buckled stage, local buckling stage and global buckling stage. In the local buckling stage, the thinner sub-laminate starts to buckle while the thicker sub-laminate keeps almost non-buckled. After this stage, the compressive behavior moves into the global buckling stage, during which the thicker sub-laminate begins to buckle and the two sub-laminates move in the same direction. In the case investigated in this paper, delaminated composite laminates almost did not experience the local buckling stage and the compressive behavior enters right into the global buckling stage, because the embedded delaminations were located near the center of plate in the thickness direction. Besides, as seen from Fig. 4 (a), (b) and (c), with the increase of delamination size, the corresponding central deflection under the same load increases.

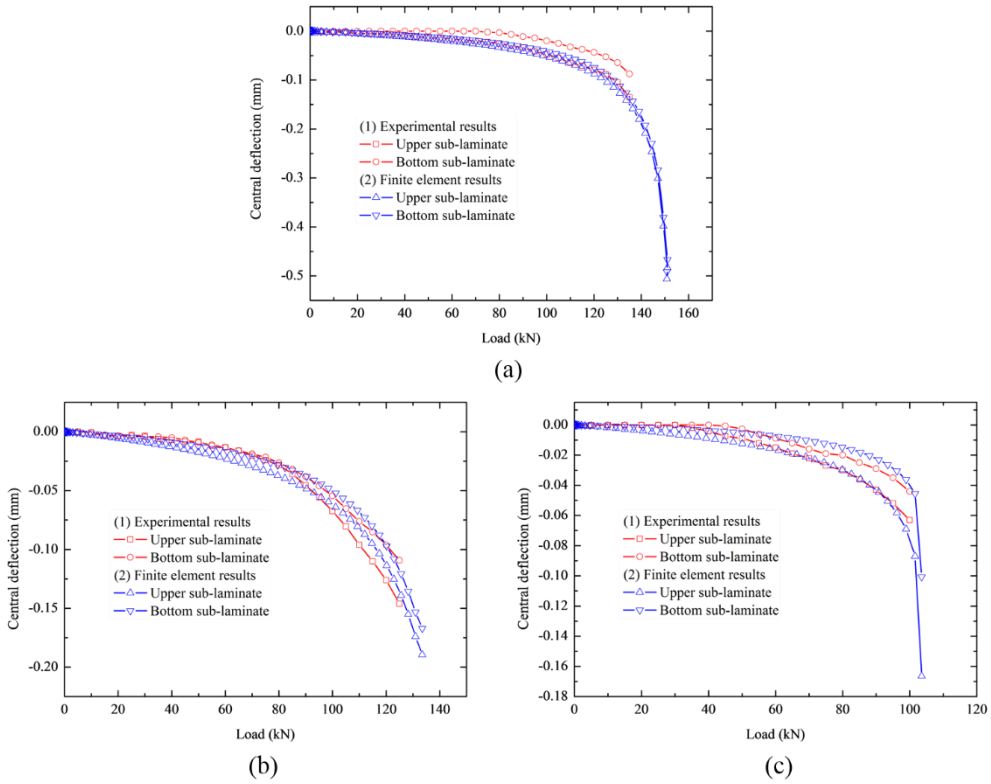

Figure 4: Load–central deflection behavior of the composite laminates.

In addition, the increase of the delamination size also leads to the change of failure mechanism. For the laminates with Φ20 mm and Φ30 mm circular delamination, with the increase of the compressive load, the buckling firstly occurred in the delaminated region, resulting in the fiber-matrix shear failure around the embedded delamination. As a consequence, the whole laminate failed without delamination growth. For the laminates with Φ50 mm circular delamination, the buckling resulted in the growth of delamination before the presence of intra-laminar failure. The delamination growth appealed perpendicular to the loading direction for a short period of time, which induced the intra-laminar failure and then leaded to the ultimate failure of the laminate rapidly. Fig. 5 (a) shows the ultrasonic C-scan testing result of delamination growth when the laminate nearly fail, in which the blue region shows the shape of the delamination and the red area is the non-damage region. Fig. 5 (b) and (c) are the FE prediction of delamination growth using different delamination growth criteria, which would be explained in detail below.

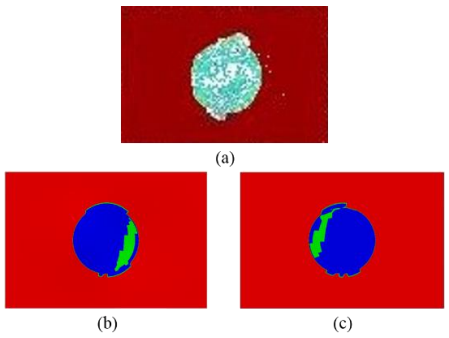

Figure 5: Experimental results and FE prediction of delamination growth.

Pietropaoli and Riccio [22] studied the compressive behavior of stiffened panels with embedded

delamination and observed that the application of the VCCT method has a severe dependency on the load step size. In order to study the sensitivity, the FE analysis of the laminates with Φ50 mm circular delamination, during which the dominant failure mechanism is the delamination growth predicted by the VCCT method, was conducted under two conditions. In the two conditions, the maximum time increments were 0.01 s and 0.005 s respectively. The initial time increment was 0.0001 s and the minimum time increment was 1e-9 s. The predicted final failure loads were about 105N and 104N, and the error was about 1%.

The load-central deflection relations of the laminates with Φ50 mm circular delamination predicted using three failure criteria are shown in Fig. 6. And the FE prediction of the delamination growth is shown in Fig. 5 where Fig. 5 (b) shows the prediction using B-K criterion and Power criterion for the parameter sets $a_m = a_n = a_o = 0.8$ and $a_m = a_n = a_o = 1.4$ while Fig. 5 (c) shows the prediction using Power criterion for the parameter set $a_m = a_n = a_o = 2.8$. Because the critical mode-II strain energy release rate is the same with mode-III SERR, the Reeder criterion could be reduced to the B-K criterion. Using the B-K or Reeder criterion, the results of the delamination growth and the load-central deflection behavior showed good agreements with the experimental results and did not change when the parameter η changed from 0.7 to 2.8. When using the Power criterion, the results of the finite element analysis were same as the results using the former two criteria for the parameter sets $a_m = a_n = a_o = 0.8$ and $a_m = a_n = a_o = 1.4$. However, for the parameter set $a_m = a_n = a_o = 2.8$, the result of the delamination growth was slightly different with the results predicted using the former two criteria, and the trend for the central deflection were steeper while the global buckling load kept almost unchanged, which would be not consistent with the experimental results. In addition, when the values of parameters a_m , a_n and a_o are below 0.8, the convergence problem emerged.

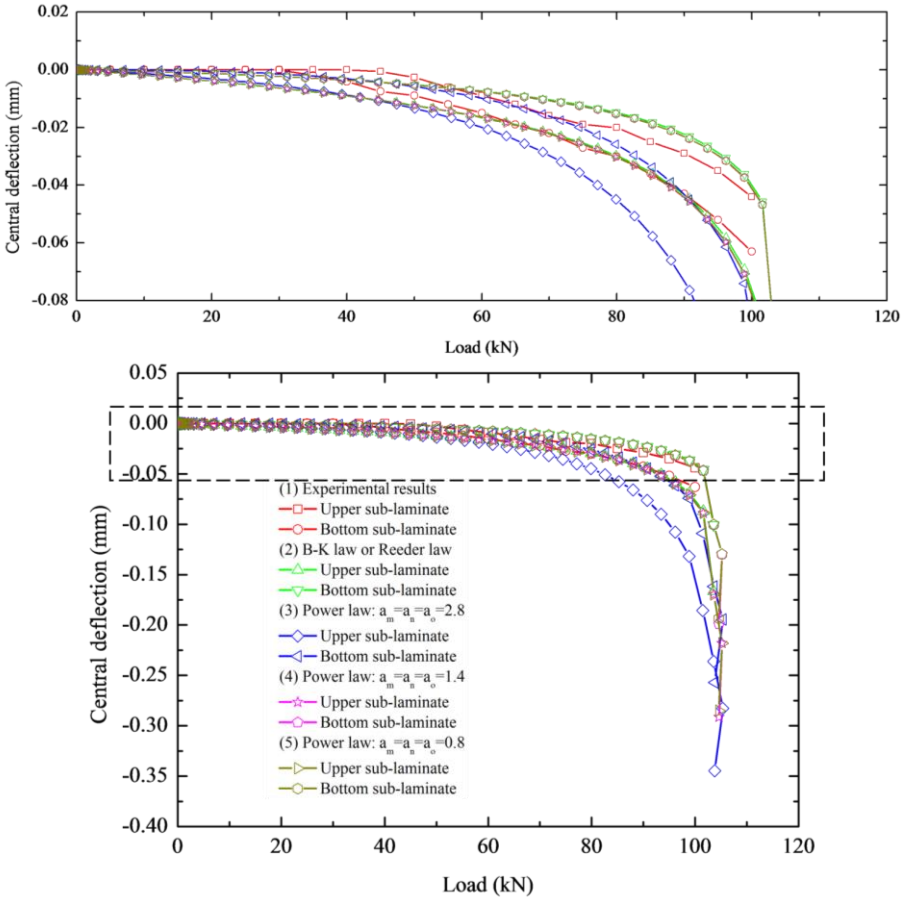

Figure 6: Load–central deflection behavior predicted using three failure criteria.

5 CONCLUSION

In this paper, the compressive behavior of composite laminates with initial delamination was investigated numerically and experimentally.

For the laminates with three different sizes of embedded delaminations, the numerical predictions including the failure load, load-center deflection relation and delamination growth of the laminates show good agreements with the experimental results, which verify the model's effectiveness. By comparing the experimental and numerical results of the laminates with different delamiantions, the significant effects of delamination size on the compressive behavior, especially on the failure mechanism, were exposed. For laminate plates with Φ20 mm and Φ30 mm circular delamination, with the increase of the compressive load, the buckling firstly occurred in the delaminated region, resulting in the fiber-matrix shear failure around the embedded delamination. As a consequence, the whole laminate failed without delamination growth. For laminate plates with Φ50 mm circular delamination, the buckling resulted in the growth of delamination, which induced the intra-laminar failure and then leaded to the ultimate failure of the laminate rapidly.

Finally, by comparing the numerical results of the plate with Φ50 mm circular delamination using three different typical failure criteria based on strain energy release rate, it was founded that the parameters of Power-law had great influence on the numerical results, while the parameters of the B-K criterion and Reeder criterion did not have significant effect on the numerical results. In addition, a sensitivity study of load step size has been conducted.

ACKNOWLEDGEMENTS

The authors would sincerely like to thank the support by the National Natural Science Funding of China (No.11372020 and 11572058).

REFERENCES

[1] Bijan Mohammadi and Farhad Shahabi, On computational modeling of postbuckling behavior of composite laminates containing single and multiple through-the-width delaminations using interface elements with cohesive law, *Engineering Fracture Mechanics*, **152**, 2015, pp. 88-104 (doi: 10.1016/j.engfracmech.2015.04.005).

[2] P.F. Liu, Z.P. Gu, X.Q. Peng and J.Y. Zheng, Finite element analysis of the influence of cohesive law parameters on the multiple delamination behaviors of composites under compression, *Composite Structures*, **131**, 2015, pp. 975-986 (doi: 10.1016/j.compstruct.2015.06.058).

[3] P.F. Liu, S.J. Hou, J.K. Chu, X.Y. Hu, C.L. Zhou, Y.L. Liu, J.Y. Zheng, A. Zhao and L. Yana, Finite element analysis of postbuckling and delamination of composite laminates using virtual crack closure technique, *Composite Structures*, **93(6)**, 2011, pp. 1549-1560 (doi: 10.1016/j.compstruct.2010.12.006).

[4] R.G. Wang, L. Zhang, J. Zhang, W.B. Liu and X.D. He, Numerical analysis of delamination buckling and growth in slender laminated composite using cohesive element method, *Computational Materials Science*, **50(1)**, 2010, pp. 20-31 (doi: 10.1016/j.commatsci.2010.07.003).

[5] Züleyha Aslan and Mustafa Şahin, Buckling behavior and compressive failure of composite laminates containing multiple large delaminations, *Composite Structures*, **89(3),** 2009, pp. 382-390(doi: 10.1016/j.compstruct.2008.08.011).

[6] Wang S and Zhang Y, Buckling, post-buckling and delamination propagation in debonded composite laminates Part 2: Numerical applications, *Composite Structures*, **88(1),** 2009, pp. 131-146(doi: 10.1016/j.compstruct.2008.02.013).

[7] A Riccio and E Pietropaoli, Modeling Damage Propagation in Composite Plates with Embedded Delamination under Compressive Load, *Journal of Composite Materials*, **42(13),** 2008, pp. 1309-1335 (doi: 10.1177/0021998308092199).

[8] Fu H and Zhang Y, On the Distribution of Delamination in Composite Structures and Compressive Strength Prediction for Laminates with Embedded Delaminations, *Applied Composite Materials*, **18(3),** 2010, pp. 253-269(doi: 10.1007/s10443-010-9154-y).

[9] H Suemasu, W Sasaki, T Ishikawa and Y Aoki, A numerical study on compressive behavior of composite plates with multiple circular delaminations considering delamination propagation, *Composites Science and Technology*, **68(12),** 2008, pp. 2562-2567(doi: 10.1016/j.compscitech.2008.05.014).

[10] R Krueger, D Goetze and J Ransom, Influence of finite element software on energy relaese rate computed using the cirtual crack closure technique, NASA/CR-2006-214523, 2006(doi: 10.1016/j.finel.2006.03.007).

[11] Krueger R, An approach to assess delamination propagation simulation capabilities in commercial finite element codes, NASA TM/2008-215123, 2008(doi: NASA/TM-2008-215123).

[12] Pavier M J and Clarke M P, Experimental techniques for the investigation of the effects of impact damage on carbon-fibre composites, *Composites Science and Technology*, **55(2),** 1995, pp. 157-169(doi: 10.1016/0266-3538(95)00097-6).

[13] Hashin Z and Rotem A, A Fatigue Failure Criterion for Fiber Reinforced Materials, *Journal of Composite Materials*, **7(4),** 1973, pp. 448-464(doi: 10.1177/002199837300700404).

[14] Hashin Z, Failure Criteria for Unidirectional Fiber Composites, *Journal of Applied Mechanics*, **47(2),** 1980, pp. 329-334 (doi: 10.1115/1.3153664).

[15] KL Reifsnider, GP Sendeckyj, SS Wang, WS Johnson, WW Stinchcomb, NJ Pagano and MN Nahas, Survey of Failure and Post-Failure Theories of Laminated Fiber-Renforced Composites, *Journal of Composites Technology and Research*, **8(4),** 1986, pp. 138-153(doi: 10.1520/CTR10335J).

[16] Hahn H T and Tsai S W, On the Behavior of Composite Laminates After Initial Failures, *Journal of Composite Materials*, **8(3),** 1974, pp. 288-305(doi: 10.1177/002199837400800306).

[17] Murray Y and Schwer L, Implementation and verification of fiber-composite damage models. Failure Criteria and Analysis in Dynamic Response, *ASME AMD*, **107,** 1990, pp. 21–30 (doi: 10.1234/12345678).

[18] Benzeggagh M L and Kenane M, Measurement of mixed-mode delamination fracture toughness of unidirectional glass/epoxy composites with mixed-mode bending apparatus, *Composites Science and Technology,* **56(4),** 1996, pp. 439-449(doi: 10.1016/0266-3538(96)00005-X).

[19] J Reeder, K Song, P Chunchu and D Ambur, Postbuckling and Growth of Delaminations in Composite Plates Subjected to Axial Compression, *43rd AIAA/ASME/ASCE/AHS/ASC structures, structural dynamics, and materials conference, Denver, Colorado, 2002,* Aiaa Journal, America, 2002, pp. 1-10.

[20] Wu E M and Reuter R C, Crack extension in fiberglass reinforced plastics, *Report No. 275, Illinois University at Urbana Dept. of Theoretical and Applied Mechanics, issue 2 ,1965,* pp. 32.

[21] Lee S Y and Park D Y, Buckling analysis of laminated composite plates containing delaminations using the enhanced assumed strain solid element, *International Journal of Solids and Structures,* **44(24),** 2007, pp. 8006-8027(doi: 10.1016/j.ijsolstr.2007.05.023).

[22] Pietropaoli E and Riccio A, On the robustness of finite element procedures based on virtual crack closure technique and fail release approach for delamination growth phenomena. Definition and assessment of a novel methodology, *Composites Science and Technology,* **70(8),** 2010, pp. 1288-1300(doi: 10.1016/j.compscitech.2010.04.006).